PHILOSOPHICAL TRANSACTIONS OF THE ROYAL SOCIETY A MATHEMATICAL, PHYSICAL & ENGINEERING SCIENCES

Condensed Phase Chemistry of Explosives and Propellants at High Temperature: HMX, RDX and BAMO [and Discussion]

T. B. Brill, P. J. Brush, P. Gray and S. A. Kinloch

Phil. Trans. R. Soc. Lond. A 1992 **339**, 377-385
doi: 10.1098/rsta.1992.0043

Condensed phase chemistry of explosives and propellants at high temperature: HMX, RDX and BAMO

By T. B. Brill and P. J. Brush

Department of Chemistry, University of Delaware, Newark, Delaware 19716, U.S.A.

By studying the behaviour of a thin film of an explosive or propellant it is possible to produce a snapshot of the surface reaction zone that exists during combustion of such explosives as cyclotrimethylene trinitramine (RDX) and cyclotetramethylene tetranitramine (HMX). Rapid heating (2000 K s^{-1}) and fast monitoring of the mass and heat-balance are performed simultaneously with fast Fourier transform infrared spectroscopic analysis of gaseous products.

Initially, HMX and RDX yield mainly N_2O at low temperatures or NO_2 at higher temperatures; the former is quickly followed by CH_2O and the latter by HCN: these species are formed from the primary residue. These concurrent pathways compensate for one another thermochemically to make this a roughly thermoneutral 'initial' stage. Subsequently, a highly exothermic reaction between CH_2O and NO_2 leads to CO, NO and H_2O and constitutes the main source of heat for the condensed phase.

The azide polymer bis(azedomethyl)oxetane has also been studied as a prototype of rather different behaviour. For it, ratios of gaseous products are not very dependent on temperature in the range 275 to 390 °C.

1. Introduction

As physical details are developed about the initiation and ignition of propellants and explosives, determination of the chemical processes under conditions of high heating rates, temperatures, and pressures is increasingly needed. Unfortunately, ignition and initiation of bulk solids involve heterogeneous phases at high pressure and temperature under dynamic, non-equilibrium conditions. The chemical details are very difficult to extract. Hence, the experimentalist is challenged to develop microscale methods that incorporate relevant conditions, but enable direct chemical studies to be made. The most convincing indication of a successful simulation is the reproduction of some key observable of a macroscale engineering test by the microscale experiment. In this way microscale chemical details can be learned about macroscale phenomena.

The quest for relevant experimental simulations has been a motivation of our laboratory. A breakthrough was recently made (Chen & Brill 1991*a*, *b*, *c*) with the SMATCH/FTIR (simultaneous mass and temperature change/Fourier transform infrared spectroscopy) method. The kinetics of fast weight loss of a thin film of material measured by this method predicted the linear burn rate of the bulk material measured at the same temperature and pressure. Hence, SMATCH/FTIR is a microscale laboratory simulation of the surface reaction zone of a burning material. The near-surface gas products are quenched and analysed in near real-time by rapid-scan IR

Phil. Trans. R. Soc. Lond. A (1992) **339**, 377–385
Printed in Great Britain

Table 1. *Comparison of calculated and measured burn rates* (mm s^{-1})

compound	SMATCH/FTIR	combustion measurement
NC	0.3	0.4
GAP	1.35	1.7
RDX	0.27	0.3
HTPB	0.21	0.19

spectroscopy. These gas products are the main reactants in the first stage of the flame zone were a flame to be present. These earliest reactants have resisted identification during actual combustion. Equally important is the discovery that the products identified by SMATCH/FTIR closely resemble those measured with our filament thermolysis methods (Oyumi & Brill 1985; Cronin & Brill 1987; Brush & Brill 1989) which are much easier to use. The connection between SMATCH/FTIR and the filament pyrolysis methods is the basis for using fast-thermolysis/FTIR spectroscopy to establish the high-temperature and high-pressure decomposition processes of bulk explosive and propellants at burning surface temperatures.

This paper describes the high temperature decomposition processes of cyclotetramethylene tetranitramine (HMX), cyclotrimethylene trinitramine (RDX) and bis(azidomethyl)oxetane polymer (BAMO) determined by the T-jump/FTIR method (Brill *et al.* 1992). However, as a backdrop, selected studies using SMATCH/FTIR are presented to support the premise that a carefully designed laboratory experiment can elucidate the chemistry that leads to ignition and the onset of explosion of an energetic material.

2. Connecting fast thermolysis to combustion

SMATCH/FTIR spectroscopy provides the dynamic weight loss, temperature change, and near-surface gas products when a 20–60 μm-thick film (0.5–1 mg) of sample is heated at a chosen rate between 100 and 350 °C s^{-1} under 1 atm† of Ar (Timken *et al.* 1990; Chen & Brill 1991*a*, *b*). Polymers, such as 13% N nitrocellulose (Chen & Brill 1991*a*), glycidylazide polymer (GAP) (Chen & Brill 1991*b*), urethane cross-linked hydroxyl-terminated polybutadiene (HTPB) (Chen & Brill 1991*c*), and crystalline monopropellants, such as HMX and RDX, have been studied. The Arrhenius parameters for the weight loss enable the regression (burn) rate of the film to be calculated from a version of the pyrolysis law. The burn rates of these materials have been measured at or extrapolated to the same temperature and pressure as the SMATCH data. The results are compared in table 1. The remarkable similarity of the data implies that SMATCH/FTIR gives a 'snapshot' of the surface reaction zone as it exists during combustion. The successful simulation of the burn rate by a microscale fast thermolysis method is central to confidence in the use of these methods to determine the heterogeneous chemistry of combusting solids.

The gas products that evolve from the film into the Ar atmosphere are detected and quantified 3 mm above the surface by rapid-scan FTIR spectroscopy. Because they are formed thermally at the same rate and temperature as combustion, the products closely relate to the reactants for the first stage of the flame zone.

It is found that simply heating a thin film of sample on a filament at a high rate

† 1 atm ≈ 10^5 Pa.

PHILOSOPHICAL TRANSACTIONS OF THE ROYAL SOCIETY A MATHEMATICAL, PHYSICAL & ENGINEERING SCIENCES

as in SMATCH/FTIR gives the same product distribution. Moreover, these simpler filament pyrolysis methods can be optimized to give information about the sequence and temperature and pressure dependence of the products. This information helps unravel the dominant chemistry of heterogeneous decomposition of the bulk material. The remainder of this article describes results of high temperature, isothermal decomposition obtained from the filament pyrolysis technique of T-jump/FTIR spectroscopy (Brill *et al.* 1992).

3. The T-jump/FTIR method

During ignition, combustion and thermal explosion of a material, the temperature at the reacting interface rises rapidly to a high temperature. Hence, thermal decomposition takes place in a temperature range considerably above that of 'slow' decomposition. The gas product distribution can be strongly affected by temperature leading to an erroneous description if the temperature factor is unknown. To establish the high-temperature chemistry, rapid heating conditions and appropriate high temperatures must be created in a microscale experiment that also enables the species to be detected.

T-jump/FTIR is a variation of the fast thermolysis/FTIR method (Oyumi & Brill 1985). A 20 μm thick Pt ribbon filament supports a thin film of material. Heating occurs at a chosen high rate up to 20000 °C s^{-1} to a chosen temperature (T_f). T_f can be maintained while the decomposition gases are analysed by rapid-scan FTIR spectroscopy. The high heating rate reduces the 'cooking' chemistry that takes place at a low heating rate. The fact that T_f is adjustable enables the products to be determined at selected temperatures including the expected burning surface temperature.

The Pt filament is an element of a very rapidly responding and sensitive bridge circuit. The control voltage of the circuit linearly responds to the Pt resistance during the programmed heating step and maintains a constant resistance once T_f is reached. The temperature of the filament is calibrated and is determined by the resistance as in a Pt thermometer. The control voltage increases or decreases very rapidly to maintain T_f in response to endothermic or exothermic events of the sample. Therefore, monitoring the control voltage as a function of time uncovers these sequential events.

A useful form of the control voltage is the difference trace (voltage without sample minus voltage with sample present) as shown in figure 1 for 200 μg of HMX. After heating at 2000 °C s^{-1} to $T_f = 298$ °C, an initial endotherm (positive deflection) occurs in the first second corresponding to melting and the higher heat capacity when sample is present. Later a sharp negative spike appears due to runaway exothermic decomposition. A heating rate of 2000 °C s^{-1} is the highest value that does not overshoot T_f. The thermal trace in figure 1 resembles a DSC thermogram, but the slope and area cannot be quantitated to obtain the reaction rate and total heat as in DSC because the rate of heat transfer between the filament and sample is not sufficiently fast. Hence the slope and area do not solely reflect the chemistry taking place. Despite this unavoidable heat transfer problem, the technique provides quasi-isothermal conditions at chosen temperatures and enables sequential thermal events and gas products to be detected at a high rate.

T-jump/FTIR has two important uses. First, the time-to-exotherm (runaway reaction, ignition, or explosion) can be determined as a function of temperature. Such

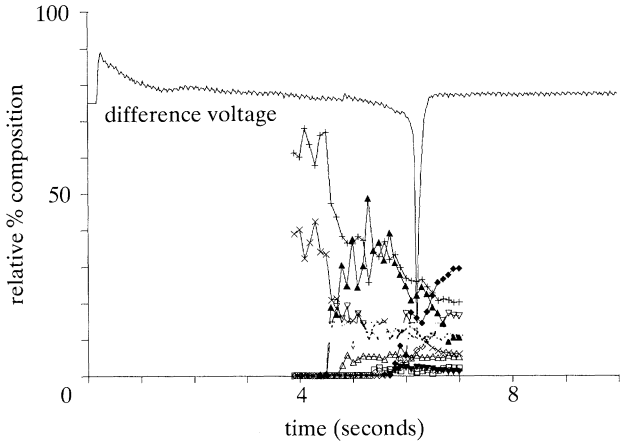

Figure 1. The thermal response trace and gas products from 200 μg of HMX heated at 2000 °C s^{-1} to 298 °C and then held at 298 °C under 2.7 atm Ar. △, % CO_2; +, % N_2O; ◆, % NO; ◇, % CO; ×, % NO_2; ▼, % HONO; ▽, % HCN; ▲, % H_2CO; □, % HNCO.

data are important for thermal explosion studies and have been acquired in other ways such as the Henkin (1952), Wenograd (1961), and ODTX (McGuire & Tarver 1981) tests. This application is briefly described in §4. Second, the IR spectra recorded simultaneously give the gas evolution sequence and relative product concentrations. These data provide insight into the decomposition mechanisms and show how the main reaction branches shift with temperature.

4. High-temperature chemistry of HMX, RDX and BAMO

(a) *HMX and RDX*

Time-to-exotherm data at several temperatures for 200 μg of HMX under 2.7 atm Ar are shown in figure 2. The slope yields the apparent activation energy, E. E is the barrier to total energy transfer rather than a particular molecular process. At lower temperatures E resembles the global decomposition E measured by DSC and TGA suggesting that the chemical processes dominate. At higher temperatures, E has a small value probably because a gas layer develops between the sample and the filament. Hence, diffusion terms as well as chemistry contribute to E. An attempt is underway to develop a heat-transfer–chemistry model for this region.

High-temperature chemistry that can be learned about explosives and propellants is the most powerful application of T-jump/FTIR spectroscopy. Insight is obtained from plots such as figure 1 determined at various temperatures. Before describing the chemistry, we note that no IR inactive products (O_2, N_2, H_2) are shown. H_2O was not quantified because of its complicated rotation–vibration fine structure. The absolute absorbance of HNCO was estimated to be half-way between that of CO_2 and N_2O. Absorbances from evaporated HMX are evident at less than 2.7 atm and for RDX at less than 4 atm. The product concentrations in figure 1 are choppy because of turbulence, incomplete mixing, and bubble bursting as the products are released. Smoothing the raw data (figure 3) is helpful. The product concentrations differ somewhat from non-isothermal high-rate decomposition (Oyumi & Brill 1985; Palopoli & Brill 1991), but the interpretations given before remain valid. The isothermal studies described here define the details more specifically over the temperature range of 290–390 °C for HMX and 260–375 °C for RDX.

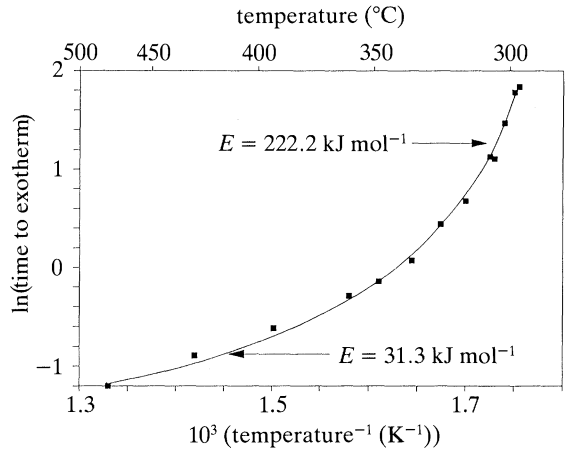

Figure 2. Time-to-exotherm for 200 μg of HMX heated at 2000 °C s^{-1} under 2.7 atm Ar.

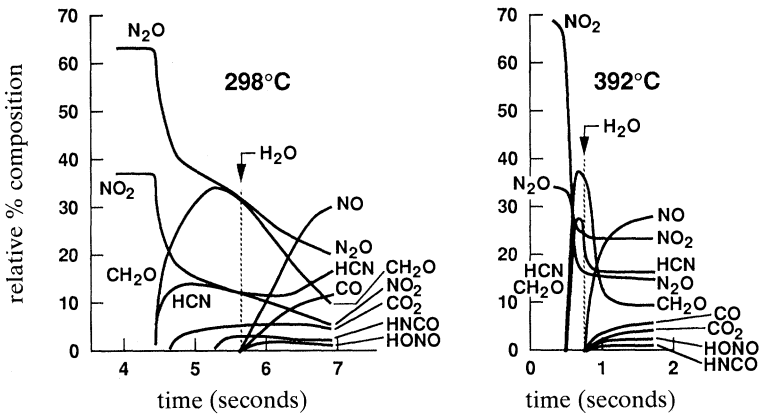

Figure 3. Smoothed gas product profiles for HMX at 298 °C (figure 1) and 392 °C.

Two global decomposition branches (4.1) and (4.2) occur for bulk RDX and HMX (Melius 1990). ΔH for the products 4(HONO + HCN) rather than 4(NO_2 + HCN + H) is given for (4.1) because a residue rather than H + HCN forms when NO_2 is released. In accordance with the sum of the ΔH for (4.1) and (4.2), the control voltage trace in figure 1 shows only slight exothermicity

$$\text{HMX} \begin{cases} \nearrow\ 4(\text{HONO}+\text{HCN}) \text{ or } 4(\text{NO}_2+\text{HCN}+\text{H}), \quad \Delta H = 159 \text{ kJ mol}^{-1}, & (4.1) \\ \searrow\ 4(\text{N}_2\text{O}+\text{CH}_2\text{O}), \quad \Delta H = -209 \text{ kJ mol}^{-1}, & (4.2) \end{cases}$$

between 4 and 5.5 s where (4.1) and (4.2) dominate. Thus, these reactions release little energy in the condensed phase. The total IR absorbance of the products accelerates from 4 to 6 s despite the constant heat flow from the filament, which implies that autocatalysis occurs.

Reactions (4.1) and (4.2) imply that N_2O and NO_2 should form simultaneously with CH_2O and HCN. This is not found at any temperature studied (e.g. figure 3). Rather, N_2O and NO_2 appear before CH_2O and HCN, which form from the residue left by elimination of N_2O and NO_2. Behrens (1990) found that N_2O forms faster than

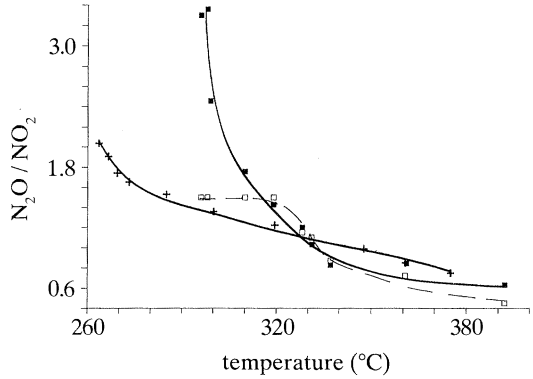

Figure 4. The temperature dependence of (4.1) and (4.2) reaction branches as measured by the N_2O/NO_2 ratio for HMX (□, initial; ■, final) and RDX (+).

CH_2O in slow heating experiments on HMX. The residue of HMX decomposition includes products like hydroxymethylformamide (HMFA) and acetamide (Cosgrove & Owen 1974; Kimura & Kubota 1980; Karpowicz & Brill 1984; Behrens 1990). These products decompose leading to delayed release of CH_2O, HCN and HNCO by (4.3) and (4.4) (Behrens 1990; Palopoli & Brill 1991).

$$\mathrm{HOCH_2NHC(O)H} \begin{cases} \nearrow \mathrm{CH_2O + HCN + H_2O}, & (4.3) \\ \searrow \mathrm{CH_2O + HNCO + 2H}. & (4.4) \end{cases}$$

At 298 °C in figure 3, the concentrations of CH_2O and HCN in the 4.5–5.5 s range match those of N_2O and NO_2 as dictated by (4.1) and (4.2).

In the vicinity of the runaway exotherm, the secondary reaction (4.5) occurs as evidenced by the fact that CH_2O and NO_2 are consumed as NO, CO and H_2O form.

$$5\mathrm{CH_2O} + 7\mathrm{NO_2} \rightarrow 7\mathrm{NO} + 3\mathrm{CO} + 2\mathrm{CO_2} + 5\mathrm{H_2O}. \quad (4.5)$$

Figure 3 shows that more NO than CO forms in accordance with (4.5). Reaction (4.5) is highly exothermic with $\Delta H = -1350$ kJ mol^{-1} and, by the large exotherm in figure 1, it is the main source of heat in the heterogeneous condensed phase. The time delay in the occurrence of (4.5) may stem from the fact that the residue and CH_2O are autocatalytic (Behrens 1990; Batten 1971). Hence, as the concentration of the residue grows, the rate of decomposition accelerates. HONO forms as CH_2O is consumed and H_2O appears suggesting that H atoms are especially free at this time in the reaction and combine with NO_2 by adventitious contact (Brill & Oyumi 1986). These conclusions also apply at 392 °C (figure 3) except that the timescale is compressed. Hence, the above decomposition process of HMX and RDX describes the 300 °C range as well as the surface reaction zone (350–400 °C) during combustion. In accordance, Shackelford *et al.* (1989) found the same kinetic isotope effect with HMX for slow decomposition and combustion.

The main change in the chemistry of HMX and RDX at different temperatures is the branching ratio of (4.1) and (4.2). Figure 4 shows the final N_2O/NO_2 concentration ratio for HMX and RDX and the initial N_2O/NO_2 ratio for HMX against temperature. The initial N_2O/NO_2 ratio is less accurate because of the low S/N ratio in the IR spectra. Clearly, (4.1) is favoured at higher temperature, while (4.2) is favoured at lower temperature. At the surface temperature of burning HMX and RDX (350–400 °C), (4.1) and (4.2) are competitive. This finding is in line with

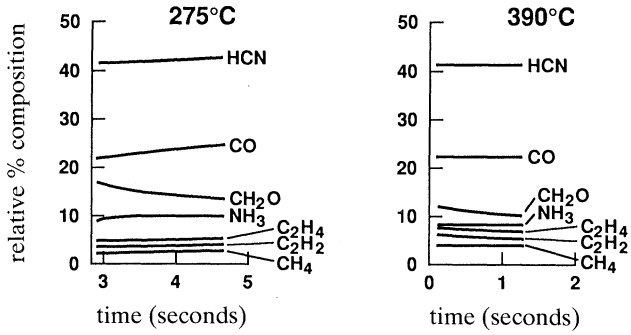

Figure 5. The gas products from BAMO at 275 °C and 390 °C showing the temperature independence of the decomposition products.

microprobe mass spectrum (MS) data of the gas ratios from burning HMX (Fetherolf *et al.* 1992). For combustion modelling the final steady state products shown in figure 3 are representative of the surface reactants for the first stage of the flame zone during combustion.

(*b*) *BAMO*

The large time and temperature dependence of the decomposition gases of HMX and RDX is not found for all energetic materials. The gas product concentrations for BAMO shown in figure 5 have little time or temperature dependence between 275 and 390 °C. N_2 is released first by the azide group, but is not detected by IR spectroscopy. The products observed come from the residual nitrene, RCH_2N. RCH_2N has two decomposition branches based on the appearance of HCN (retention of C–N bond) and NH_3 (cleavage of C–N bond). The high concentration of HCN indicates that (4.6) is favoured.

$$RCH_2N \nearrow \text{HCN} + \text{hydrocarbons}, \tag{4.6}$$

$$\searrow \text{NH}_3 + \text{hydrocarbons}. \tag{4.7}$$

However, according to figure 5 the branching ratio and overall reactions are independent of temperature in the range studied.

5. The effect of pressure

The pressure dependence of the final gas product concentrations from isothermal decomposition of HMX at 300 °C and 360 °C was determined. Figure 6 gives the 360 °C data under 1–27 atm Ar. Similar studies under non-isothermal conditions are confirmed by figure 6 (Oyumi & Brill 1987). At 1 atm the most reactive gases (NO_2, CH_2O and HONO) have their highest residual concentration. At 2.7 atm, NO_2 and HONO react to a greater extent with CH_2O yielding CO and NO. Under 6.7 atm these conversions are sufficiently complete that no NO is detected in the timescale of the experiment. N_2 is the main nitrogen containing product. This pattern results from increased heterogeneous gas phase-condensed phase chemistry at higher pressure, because the diffusion of gas products away from the filament-sample zone is suppressed. The longer residence time in this high temperature zone advances the reaction scheme. Hence, the global nitrogen and carbon schemes of $NO_2 \rightarrow NO \rightarrow N_2$ and $CH_2O \rightarrow CO(CO_2)$ shift to the right at higher pressure. There is no evidence of a change in the decomposition mechanism in this pressure range.

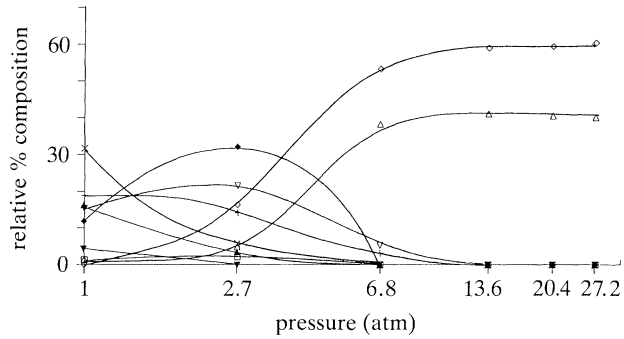

Figure 6. The dependence on the static Ar pressure of the final gas product concentrations from HMX heated at 2000 °C s^{-1} to 360 °C. See figure 1 for key to symbols.

We are grateful to the U.S. Air Force Office of Scientific Research, Aerospace Sciences for support of this work.

References

Batten, J. J. 1971 The thermal decomposition of RDX at temperatures below the melting point. *Aust. J. Chem.* **24**, 2025–2029.

Behrens, R. Jr. 1990 Thermal decomposition of energetic materials. Temporal behaviors of the rates of formation of the gaseous pyrolysis products of HMX. *J. Phys. Chem.* **94**, 6706–6718.

Brill, T. B. & Oyumi, Y. 1986 Thermal decomposition of energetic materials 17. A relationship of molecular composition to HONO formation. *J. phys. Chem.* **90**, 6848–6853.

Brill, T. B., Brush, P. J., James, K. J., Shepherd, J. E. & Pfeiffer, K. J. 1992 *Appl. Spectrosc.* (In the press.)

Brush, P. J. & Brill, T. B. 1989 Chemical phenomena associated with the initiation of thermal explosions. In *Proc. Ninth Symp.* (*Int.*) *on Detonation*, pp. 228–234. Office of Naval Research, U.S.A.

Chen, J. K. & Brill, T. B. 1991*a* Thermal decomposition of energetic materials 50. Kinetics and mechanism of nitrate ester polymers at high heating rates by SMATCH/FTIR spectroscopy. *Combust. Flame* **85**, 479–488.

Chen, J. K. & Brill, T. B. 1991*b* Thermal decomposition of energetic materials 54. Kinetics and near-surface products of AMMO, BAMO and GAP in simulated combustion. *Combust. Flame* **87**, 157–168.

Chen, J. K. & Brill, T. B. 1991*c* Chemistry and kinetics of hydroxyl-terminated polybutadiene (HTPB) and diisocyanate-HTPB polymers during slow decomposition and combustion. *Combust. Flame* **87**, 217–232.

Cosgrove, J. D. & Owen, A. J. 1974 The thermal decomposition of 1,3,5 trinitrohexahydro 1,3,5 triazine (RDX) – Part I. The products and physical parameters. *Combust. Flame* **22**, 13–18.

Cronin, J. T. & Brill, T. B. 1987 Thermal decomposition of energetic materials 26. Simultaneous temperature measurements of the condensed phase and rapid-scan FTIR spectroscopy of the gas phase at high heating rates. *Appl. Spectrosc.* **41**, 1147–1151.

Fetherolf, B. L., Liiva, P. M., Litzinger, T. A. & Kuo, K. K. 1992 Thermal and chemical structure of the preparation and reaction zones for RDX and RDX composite propellants. In *Proc. 28th JANNAF Combust. Meeting*. Chemical Propulsion Information Agency.

Henkin, H. & McGill, R. 1952 Rates of explosive decomposition of explosives. *Ind. Eng. Chem.* **44**, 1391–1395.

Karpowicz, R. J. & Brill, T. B. 1984 *In situ* characterization of the "melt" phase of RDX and HMX by rapid-scan FTIR spectroscopy. *Combust. Flame* **56**, 317–325.

Kimura, J. & Kubota, N. 1980 Thermal decomposition process of HMX. *Prop. Explos.* **5**, 1–8.

Melius, C. F. 1990 *Chemistry and physics of energetic materials* (ed. S. Bulusu), pp. 21–50. Dordrecht: Kluwer.

PHILOSOPHICAL TRANSACTIONS OF THE ROYAL SOCIETY A MATHEMATICAL, PHYSICAL & ENGINEERING SCIENCES

McGuire, R. R. & Tarver, C. M. 1981 Chemical decomposition models for the thermal explosion of confined HMX, TATB, RDX and TNT explosives. In *Proc. Seventh Symp.* (*Int.*) *on Detonation*, pp. 56–64.

Oyumi, Y. & Brill, T. B. 1985 Thermal decomposition of energetic materials 3. A high-rate, *in situ* FTIR study of the thermolysis of HMX and RDX with pressure and temperature as variables. *Combust. Flame* **62**, 213–224.

Oyumi, Y. & Brill, T. B. 1987 Thermal decomposition of energetic materials 22. The contrasting effects of pressure on the high-rate thermolysis of 34 energetic compounds. *Combust. Flame* **68**, 209–216.

Palopoli, S. F. & Brill, T. B. 1991 Thermal decomposition of energetic materials 52. On the foam zone and surface chemistry of rapidly decomposing HMX. *Combust. Flame* **87**, 45–60.

Shackelford, S. A., Goshgarian, B. B., Chapman, R. D., Askins, R. E., Flanigan, D. A. & Rogers, R. N. 1989 Deuterium isotope effects during HMX combustion: Chemical kinetic burn rate control mechanism verified. *Prop. Explos. Pyrotech.* **14**, 93–102.

Timken, M. D., Chen, J. K. & Brill, T. B. 1990 Thermal decomposition of energetic materials 37. SMATCH/FTIR spectroscopy. *Appl. Spectrosc.* **44**, 701–706.

Wenograd, J. 1961 The behaviour of explosives at very high temperatures. *Trans. Faraday Soc.* **57**, 1612–1620.

Discussion

P. Gray (*Cambridge University, U.K.*). These novel techniques permit much greater assurance about probable pathways. I would like to suggest that although the NO_2 and perhaps the N_2O are primary products, these atomic groupings being present in the reactants, the CH_2O and HCN follow them in time. The exothermic reaction between CH_2O and NO_2 goes back many years, and I believe that it offers, via HONO, the main route to NO.

In the BAMO case the mono- and di-nitrenes are the plausible precursors and these species are not only notoriously reactive but may offer routes to reaction-chain branching (autocatalysis). Interestingly, that first step:

$$\text{azide} \rightarrow \text{nitrene} + \text{nitrogen}$$

is not a source of great energy. The subsequent reactions of the nitrenes, however, will release much heat.

S. A. Kinloch (*RMCS, Shrivenham, U.K.*). You stated that the first stage of the decomposition process in these experiments, in which production of NO_2 and N_2O is witnessed, is thermally neutral because the two reaction pathways are thermodynamically opposite in character and approximately cancel each other. You later showed that the dominance ratio of the two reaction pathways could vary between approximately 0.6 and 3.5. Is the net endothermic or exothermic behaviour produced by this variation of sufficient magnitude to be reflected in the control voltage signal?

T. B. Brill. The control voltage traces in the first stage are, indeed, somewhat more exothermic at lower temperature than at higher temperature. However, the differences are close to the limit of the sensitivity of the control voltage circuit.